

Mitigating Hallucinations in Large Vision-Language Models with Internal Fact-based Contrastive Decoding

Chao Wang^{† 1 2} Xuancheng Zhou^{1 2} Weiwei Fu^{1 2} Yang Zhou^{† 2 3}

Abstract

Large Visual Language Models (LVLMs) integrate visual and linguistic modalities, exhibiting exceptional performance across various multimodal tasks. Nevertheless, LVLMs remain vulnerable to the issue of object hallucinations. Previous efforts to mitigate this issue focus on supervised fine-tuning (SFT) or incorporating external knowledge, both of which entail significant costs related to training and the acquisition of external data. To address these challenges, we propose a novel model-agnostic approach termed Internal Fact-based Contrastive Decoding (IFCD), designed to mitigate and suppress hallucinations during the inference process of LVLMs by exploiting the LVLMs' own hallucinations. IFCD is grounded in experimental observations that alterations to the LVLMs' internal representations tend to amplify hallucinations caused by language bias. By contrasting disturbed distribution, IFCD calibrates the LVLMs' output and effectively removes the hallucinatory logits from the final predictions. Experimental results validate that IFCD significantly alleviates both object-level and attribute-level hallucinations while achieving an average 9% accuracy improvement on POPE and 8% accuracy improvement on MME object hallucinations subset compared with direct decoding, respectively.

1. Introduction

In recent years, significant advancements have been made in developing large vision-language models (LVLMs) (Li et al., 2023b; Wen et al., 2024), which exhibit exceptional capabilities across a broad spectrum of tasks (Achiam et al.,

[†]Corresponding Author. ¹School of Future Technology, Shanghai University, Shanghai, 200444, China. ²Institute of Artificial Intelligence, Shanghai University, Shanghai, 200444, China. ³School of Mechatronic Engineering and Automation, Shanghai, 200444, China. Correspondence to: Chao Wang <cwang@shu.edu.cn>, Yang Zhou <saber_mio@shu.edu.cn>.

Under review.

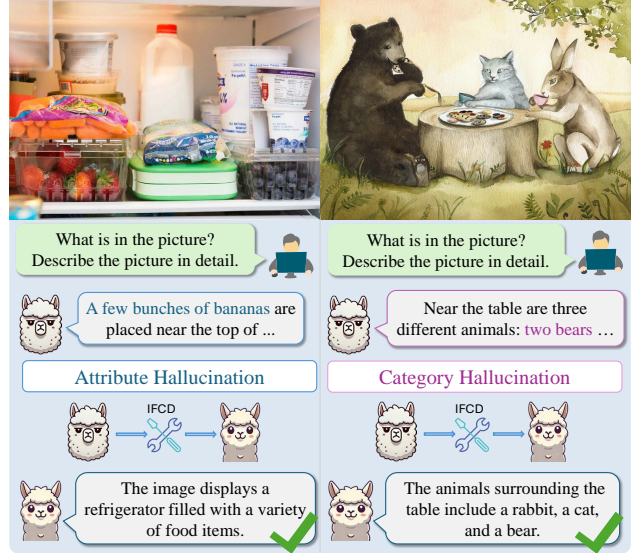


Figure 1. Cases of object hallucinations and effect of IFCD on LLaVA 1.5. Given two images, an LLaVA 1.5 outputs responses with attribute and category hallucinations which IFCD fixes.

2023). These models are increasingly viewed as a step toward achieving artificial general intelligence (Sanderson, 2023). LVLMs are capable of extracting intricate complex visual information and transforming it into continuous language representations for generation (Liu et al., 2024; Zhu et al., 2024). However, a critical challenge that persists with LVLMs is the phenomenon of hallucinations. Before the era of LVLMs, the natural language processing (NLP) community defined hallucinations as generated textual content that deviates from actuality (Ji et al., 2023; Biten et al., 2022). With the advancements of LVLMs, a new form of hallucination has emerged, known as object hallucination. This refers to the generation that are inconsistent with visual input, and it becomes a significant issue that impedes the deployment of LVLMs in domains that require high reliability, particularly in risk-sensitive industries (Sahoo et al., 2024).

Object hallucinations refer to the phenomenon where the language output generated by an LVLM fails to align with the visual input content (Song & Huang, 2024; Min et al., 2024). In Figure 1, the LVLM incorrectly assumes that bananas are present in the refrigerator and even provides a

false location of the bananas. At the same time, the LVLM accurately counts the number of animals but misclassifies an animal that is not a bear as a bear in another example. These two examples highlight the object hallucinations issue in LVLMs, which severely limits their applicability in domains where high accuracy is essential (Zhang et al., 2023; Pal et al., 2023). Therefore, addressing the object hallucinations is a pivotal step toward enhancing the reliability of LVLMs and expanding their potential applications.

To address the issue of object hallucinations in LVLMs, numerous works focus on incorporating external information to support fact-checking (Zhao et al., 2024; Asai et al., 2023), thereby enhancing the factual accuracy of LVLMs through techniques such as self-evaluation (Singhal et al., 2024). Additionally, improving LVLMs performance through preference fine-tuning is a prevalent strategy (Rafailov et al., 2024; Stiennon et al., 2020), aiming to align model outputs with human preferences and enhance model performance at a fine-grained level. While existing interventions for mitigating object hallucinations in LVLMs have shown effectiveness, the associated human and computational costs highlight the urgent need for simpler yet effective approaches.

To address these challenges, we propose Internal Fact-based Contrastive Decoding (IFCD), a novel model-agnostic approach that leverages hallucinations to mitigate further hallucination. IFCD can be seamlessly integrated into any open-source LVLM with minimal training required for the probe model. IFCD significantly enhances the truthfulness of LVLMs while reducing object hallucination. To assess the effectiveness of IFCD, we conduct experiments on two widely adopted LVLMs, LLaVA 1.5 (Liu et al., 2024) and InstructBLIP (Li et al., 2023a). Our evaluation using the Polling-based Object Probing Evaluation (POPE) (Li et al., 2023d) demonstrates that IFCD consistently outperforms baseline approaches, achieving up to a 9% improvement in performance across all LVLMs. Additionally, IFCD enhances the overall perceptual capabilities of LVLMs, as evidenced by benchmarking on MME (Fu et al., 2023) and LLaVA-Bench (Liu et al., 2024). In the text generation task, IFCD reduces the hallucinated object ratio by 5%, while preserving the generated text’s quality.

Concretely, our main **contributions** are as follows: **1).** We analyze the impact of editing internal representations on object hallucinations in LVLMs, with a particular focus on the effects of language bias. **2).** We introduce IFCD, a novel technique to calibrate LVLMs’ output distribution and mitigate object hallucinations by contrasting the disturbed distribution derived from internal representation editing. **3).** IFCD demonstrates the effect in mitigating object hallucination, achieving 9% and 8% improvement on POPE and MME, respectively, and 13% improvement in suppressing

hallucinatory object effects while being more robust in the long text generation experiments.

2. Related Work

2.1. Large Visual Language Models

In recent years, large language models (LLMs) based on the Transformer architecture have achieved remarkable achievements in various fields, including Natural Language Processing (NLP), Machine Translation, and Computer Vision. (Zhao et al., 2023; Achiam et al., 2023; Chiang et al., 2023). Notably, with the introduction of multimodal models such as CLIP (Radford et al., 2021) and Vision Transformer (Dosovitskiy et al., 2021), LVLMs have been established through comprehensive pre-training processes that unify textual and visual modalities (Bai et al., 2023; Ye et al., 2024a). Compared with traditional vision models, LVLMs adopted more advanced training paradigms (Wei et al., 2022; Liu et al., 2024). As a result, LVLMs demonstrated unique capabilities not present in traditional models (Yang et al., 2023), including establishing application (Ye et al., 2024a), and advanced mathematical reasoning (Driess et al., 2023).

2.2. Object Hallucination

While LVLMs exhibited strong capabilities in addressing vision-language tasks, they were still significantly affected by object hallucinations (Li et al., 2023d), generating content irrelevant to visual information. To identify the issue of object hallucinations in LVLMs, recent research has established specific indicators, such as Caption hallucinations Assessment with Image Relevance (CHAIR) (Rohrbach et al., 2018) and Sharpness (Chen et al., 2024a). Additionally, advances have been made in locating the causes of hallucinations within LVLMs, including internal representation and attention patterns (Han et al., 2024; Mahaut et al., 2024). These metrics and locating approaches provided a multi-dimensional view to observe object hallucination.

Addressing object hallucinations typically focused on direct suppression methods and fine-tuning, which involved actively limiting (Dhuliawala et al., 2024), correcting hallucinated outputs (Hu et al., 2024) and RLHF to refine LVLMs (Ye et al., 2024b). These approaches often constructed enhanced datasets for fine-tuning or training LVLMs. As the parameter scales of LVLMs continued to increase, these challenges became even more pronounced (Ye et al., 2024a; Zhu et al., 2024). To tackle these issues, IFCD actively induces hallucinations into the model’s output and leverages them as counterexamples to refine the model’s final responses, thereby reducing the likelihood of hallucinations in final outputs. IFCD leverages hallucinated outputs as improving opportunities, offering a novel way to mitigate object hallucinations without high computation costs.

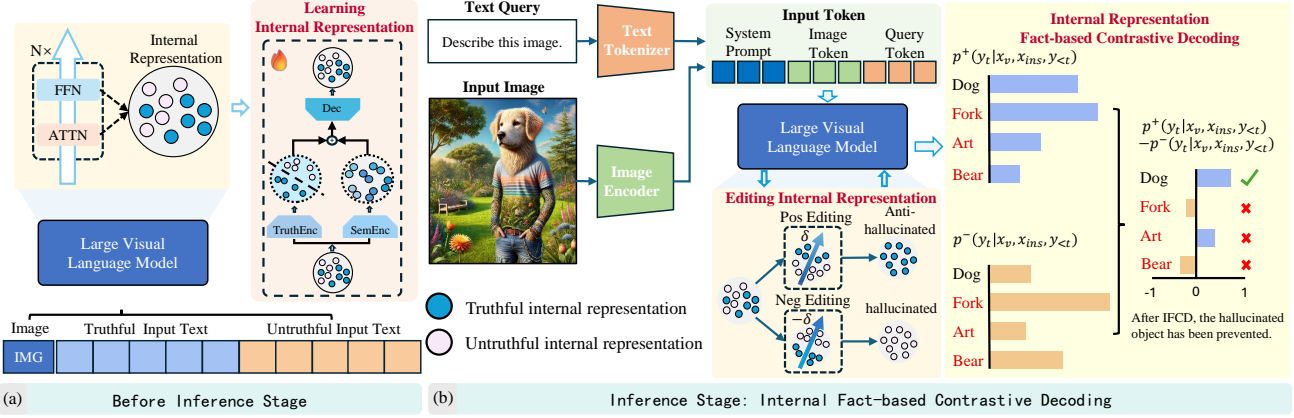


Figure 2. An overview of IFCD. IFCD first edits the internal representation of the LVLMs to construct counterfactual logits for comparison by deliberately injecting hallucinations into the model trained by contrastive learning. These counterfactual logits are utilized to reveal potential hallucinatory tendencies of the LVLMs. Furthermore, the internal representation editing model is employed to actively attenuate a portion of the hallucinatory components within the LVLMs, thereby initiating an improvement in the factual accuracy of its outputs. This process effectively corrects the token from an erroneous token “[Fork]” to an accurate “[Dog]”.

3. Method

3.1. Overview

In this section, we propose IFCD to mitigate object hallucinations in LVLMs effectively. IFCD constructs two distributions with a truthfulness gap via internal representation editing and mitigates object hallucinations using contrastive decoding to subtract hallucinatory distributions. Section 3.2 details the editing process, while Section 3.3 explains the contrastive decoding mechanism. The overall framework is illustrated in Figure 2.

3.2. Amplifying Object hallucinations via Internal Representation Editing

Induction of Object hallucinations A substantial proportion of object hallucinations arises from statistical bias (Zhao et al., 2024), for which contrastive decoding has emerged as an effective countermeasure (Chen et al., 2024c; Min et al., 2024). The methodology originates from contrastive decoding (Li et al., 2023c), which subtracts logits that deviate from expected distributions, thereby enhancing the performance of LVLMs. Existing approaches reveal LVLMs’ tendency toward object hallucinations by confusing the visual input (Leng et al., 2024) or instructing LVLMs to make incorrect decisions (Wang et al., 2024) and mitigate hallucinations via contrastive decoding. Therefore, a critical question arises: *How can we create hallucination-inducing samples that reflect token distribution errors while generating significant hallucination?*

We argue that previous methods relying on distracting information are suboptimal for inducing object hallucinations in

LVLMs. These approaches primarily highlight the models’ reactions to specific commands or perturbations. Although these responses approximate object hallucination, they stem from exogenous factors rather than inherent model errors and hardly fully represent LVLMs’ object hallucination. To better simulate logits indicative of object hallucination, we propose intervening in the internal representation of LVLMs during inference.

Introduction of Internal Representation Editing Intuitively, the internal representations from the attention and feedforward layers directly contribute to the inference process, thereby influencing the model’s output. This section delves into an analysis aiming to validate the hypotheses that editing internal representation can amplify object hallucinations in LVLMs. There are various methods to intervene in internal representations to alter output truthfulness (Pan et al., 2024; Chen et al., 2024b). Considering compatibility and availability, we propose using TruthX (Zhang et al., 2024) to edit the internal representations of LVLMs. TruthX is an autoencoder-based model comprising two encoders, TruthEnc(\cdot) and SemEnc(\cdot), and a decoder Dec(\cdot), all implemented with multi-layer perceptions (MLPs). Two encoders map LVLMs’ internal representations x as follows:

$$h_{truth} = \text{TruthEnc}(x), h_{sem} = \text{SemEnc}(x), \quad (1)$$

where $h_{truth}, h_{sem} \in \mathbb{R}^{d_{latent}}$ are the latent representations in the latent spaces of TruthEnc(\cdot) and SemEnc(\cdot), d_{latent} is the dimension of latent space. Then decoder Dec(\cdot) reconstructs LVLM internal representation:

$$x' = \text{Dec}(h_{sem} + \text{Attn}(h_{sem}, h_{truth})), \quad (2)$$

where x' is the reconstructed representation and Attn(\cdot) is

an attention operation from semantic latent representation to truthful latent representation.

Internal Representation Editing Amplifies Object hallucinations Through contrastive learning, the truthfulness of the LVLMs’ internal representation can be discerned within $\text{TruthEnc}(\cdot)$. The editing procedure is subsequently determined by the relative positions of the central point of the latent space vectors corresponding to truthful and untruthful representations mapped by $\text{TruthEnc}(\cdot)$. Formally, the direction $\delta \in \mathbb{R}^{d_{latent}}$ of internal representation editing can be defined as follows:

$$\delta = \bar{\mathcal{H}}_{truth}^{pos} - \bar{\mathcal{H}}_{truth}^{neg}, \quad (3)$$

where $\bar{\mathcal{H}}_{truth}^{pos}$ and $\bar{\mathcal{H}}_{truth}^{neg}$ denotes the average position of mappings of truthful and untruthful representations within the latent space of $\text{TruthEnc}(\cdot)$. Note that the determination of editing direction δ happens during the training stage of TruthX. Adjustments to truthfulness can be reversed if the opposite direction $-\delta$ is used.

In the inference process of the LVLMs, TruthX maps and edits the internal representation in the latent space of $\text{TruthEnc}(\cdot)$, then reconstructs the internal representation. Through contrasting the difference between the original and reconstructed internal representation, the content of the modifications to the internal representation $\Delta \in \mathbb{R}^{d_{model}}$ can be effectively derived, where d_{model} refers to the dimension of LVLMs internal representations.

Then, the internal representation x of LVLMs is edited as follows formally:

$$\hat{x} = x + \gamma \times \Delta, \quad (4)$$

where γ denotes the editing strength and \hat{x} is the reconstructed internal representation of LVLMs. In practice, it is not necessary to edit all attention and feedforward layers. Modifying the layers that are sensitive to factual differences alone can yield substantial change in object hallucination.

We compare the effect of editing the internal representation of LVLMs to expose object hallucinations preference with two alternative interference methods, using the case of recognizing black strawberries on LLaVA 1.5 in Figure 3. For Instruction Disturbance, we follow Instruction Contrastive Decoding (Wang et al., 2024), utilizing the prompt “You are a confused object detector.” to induce hallucination. For visual disturbance, we adopt the methodology from Visual Contrastive Decoding (Leng et al., 2024), setting the noise step parameter to 400, which controls the scale of noise added. Figure 3 presents editing the internal representation enables the LVLMs to disregard visual information and disproportionately rely on language priors in its decision-making process. Additionally, increasing the strength of the internal representation modification can further expose the statistical bias in the responses.

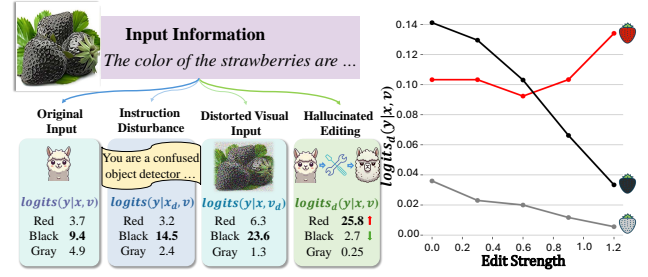


Figure 3. An illustration of editing internal representation amplifying language priors. Given an image depicting three black strawberries, LVLMs assign more preference for more conventional strawberry color, such as “red”, with increasing editing strength.

3.3. Internal Fact-based Contrastive Decoding

Contrasting the Predictions with Disturbance The findings from our previous analyses substantiate the hypothesis that *manipulating the internal representations of LVLMs can exacerbate object hallucination, thereby making hallucinatory content more strongly reflective of untruthful information*. A promising approach to mitigate object hallucinations of LVLMs is to directly subtract the logits associated with hallucinatory content from the final output logits, thereby enabling a more targeted mitigation of object hallucination. Building upon this view, we introduce IFCD aimed at alleviating hallucinations during LVLMs inference.

Drawing from the concept of contrastive decoding (Li et al., 2023c), which enhances the overall quality of LLM outputs by comparing logits from two models with performance discrepancies, we contrast the generations from the hallucination-inducing and hallucination-suppressing models to improve final performance. Specifically, as demonstrated in Figure 2, given the visual features X_v extracted from the visual encoder and the textual query X_q , our method computes two distinct token distributions: the first distribution P^+ is derived from the LVLM edited for anti-hallucination. In contrast, the second distribution P^- is generated from the LVLM after modification of its internal representations for hallucination-inducing. In contrast to the regular approach of selecting the token with the highest probability, our method relies on the two token distributions, P^+ and P^- , to inform the final token selection. The contrasting token probability distribution is computed by evaluating the difference between P^+ and P^- as follows:

$$p_{\text{IFCD}}(y_t|x_v, x_q) = \sigma \left((1 + \alpha)p^+(y_t|*) - \alpha p^-(y_t|*) \right), \quad (5)$$

where $*$ denotes visual and textual information given to LVLMs as well as previously generated tokens, while α is employed to control the contrast strength, and y_t refers to the token generated in t -th position.

Adaptive Plausibility Constraints The fundamental principle of IFCD is to prioritize the selection of tokens with high probabilities as predicted by the LVLMs, while simultaneously imposing penalties on those tokens associated with hallucinatory logits. However, this approach risks inadvertently affecting tokens that are correctly identified both under standard conditions and hallucinated content. Imposing penalties on these tokens may inadvertently reward unreliable tokens that should not be prioritized, potentially distorting the LVLMs’ output. To mitigate this issue, we introduce constraints on the scope of influence exerted by IFCD, drawing upon adaptive plausibility constraints that are employed in the open-ended text generation realm (Li et al., 2023c).

$$y_t \sim P_{\text{IFCD}}, \text{s.t. } y_t \in \mathcal{V}_{\text{head}}(y_{<t}), \quad (6)$$

$$\mathcal{V}_{\text{head}}(y_{<t}) = \{y_t \in \mathcal{V} : p(y_t|*) \geq \beta \max_{[\mathcal{T}]} p([\mathcal{T}]|*)\}, \quad (7)$$

where $[\mathcal{T}]$ refers to the candidate tokens, while the pivotal hyperparameter β serves to regulate the truncation strength of the logits, thereby determining the tokens affected during the contrastive decoding process. This parameter is crucial for constraining the impact on irrelevant tokens, thereby ensuring the robustness of the contrastive decoding process.

4. Experiments

4.1. Experiments Settings

Benchmarks **POPE** (Li et al., 2023d) comprises 1,500 images from three sources—MSCOCO, A-OKVQA, and GQA—along with 27,000 associated questions, focusing on detecting object existence hallucination. It also incorporates three sampling methods—random, popular, and adversarial—to evaluate the robustness of LVLMs against object hallucinations driven by statistical biases. **MME** (Fu et al., 2023) provides a total of 14 perception and cognition tasks. Since the cognitive task is related to the language decoder’s reasoning capacity rather than visual content comprehension, we choose the perceptual subset of MME as the benchmark. Among these tasks, *existence, count, position, and color* tasks are specifically designed as hallucinations discrimination benchmarks. **MSCOCO** (Lin et al., 2014) is a widely used computer vision benchmark, which contains more than 200,000 manually labeled high-quality and complex image-captions pairs, therefore very suitable for evaluating the object hallucinations problem. We randomly selected 500 images from MSCOCO to validate the long text generation ability of our method. **LLaVA-Bench** (Liu et al., 2024) contains 24 images with 60 questions, and the images cover a range of content such as portraits, landscapes, and enigmatic causes. We conduct a case study with this dataset to qualitatively demonstrate the effectiveness of our proposed IFCD.

Metrics The POPE evaluation pivots four key metrics: Accuracy, Precision, Recall, and the F1 score. To MME, we quantify performance via official implementation, the combined metric of accuracy and accuracy+. MSCOCO tests text generation capacity, which is quantified by BLEU (Papineni et al., 2002) and CHAIR (Rohrbach et al., 2018). Specifically, CHAIR contains two sub-metrics CHAIR_i and CHAIR_s , for object-focused and sentence-focused levels respectively. Formally, CHAIR_i and CHAIR_s could be described as follows:

$$\text{CHAIR}_i = \frac{|\{\text{hallucinated objects}\}|}{|\{\text{all objects mentioned}\}|}, \quad (8)$$

$$\text{CHAIR}_s = \frac{|\{\text{sentences with hallucinated object}\}|}{|\{\text{all sentences}\}|},$$

LVLMs Baselines We evaluate the effectiveness of IFCD on two popular LVLMs, LLaVA 1.5 (Liu et al., 2024) and InstructBLIP (Li et al., 2023a), configured with Vicuna 7B as the language decoder. Additionally, we reproduce the widely recognized Visual Contrastive Decoding (VCD) (Leng et al., 2024) and Instruction Contrastive Decoding (ICD) (Wang et al., 2024) as comparisons with IFCD. Through comprehensive experiments, we demonstrate that IFCD is model-agnostic and can be seamlessly integrated with various LVLM architectures.

Implementation Details In the experiments, we follow all hyperparameter settings in Appendix B unless otherwise noted. We use 300 MSCOCO images paired with both correct and incorrect responses as the training dataset for TruthX. We demonstrate and discuss the performance of IFCD with different training sizes in Appendix A. When adjusting the internal representations of LVLMs, we modify only the top 15 most important layers, with the editing strength $s = 0.5$. It is worth noting that all experiments were conducted on a single RTX 3090 (24GB), highlighting the low cost of implementing IFCD.

4.2. Experimental Results

Results on POPE We use POPE to assess whether LVLMs misinterpret image objects. By applying different sampling methods in POPE, we can further evaluate the effectiveness of various methods in addressing statistical bias. As shown in Table 1, two LVLMs employed IFCD achieve average accuracy improvements of up to 6.22 and 7.69, respectively, and F1 score improvements of up to 7.14 and 7.62, respectively, compared to the direct decoding, demonstrating the effectiveness of IFCD. A notable observation is that *the different POPE setting varies the performance of all LVLMs with all methods, which could confirm the research that statistic bias is a cause of object hallucination* (Zhou et al., 2023). However, among the four decoding methods, the performance degradation from the random setting to the adversarial setting is smaller for IFCD compared to the others.

Table 1. Results on object hallucinations benchmark POPE. Regular denotes direct sampling, whereas ICD and VCD are two baselines for comparison, and IFCD is our proposed decoding. The best performance is marked by **bold**, and performance of IFCD is marked by [cyan](#).

DATASET	SETTING	DECODING	LLAVA 1.5				INSTRUCTBLIP			
			ACCURACY	PRECISION	RECALL	F1 SCORE	ACCURACY	PRECISION	RECALL	F1 SCORE
MSCOCO	RANDOM	REGULAR	83.29	92.13	72.80	81.33	80.71	81.67	79.19	80.41
		ICD	84.23	95.08	72.20	82.08	83.50	87.69	77.93	82.52
		VCD	87.73	91.42	83.28	87.16	84.53	88.55	79.32	83.68
		IFCD (OURS)	89.17	94.54	83.13	88.47	85.56	97.09	73.33	83.75
	POPULAR	REGULAR	81.88	88.93	72.8	80.06	78.22	77.87	78.85	78.36
		ICD	82.73	91.47	72.20	80.70	79.40	80.28	77.93	79.09
		VCD	85.38	86.92	83.28	85.06	81.47	82.89	79.32	81.07
		IFCD (OURS)	88.10	93.13	82.27	87.36	83.27	91.93	72.93	81.34
A-OKVQA	ADVERSARIAL	REGULAR	78.96	83.06	72.75	77.57	75.84	74.30	79.03	76.59
		ICD	80.23	85.96	72.27	78.52	77.70	77.57	77.93	77.75
		VCD	80.88	79.45	83.29	81.33	79.56	79.67	79.39	79.52
		IFCD (OURS)	85.17	86.76	83.00	84.84	82.23	89.47	73.07	80.44
	RANDOM	REGULAR	83.45	87.24	78.36	82.56	80.91	77.97	86.16	81.86
		ICD	86.13	91.44	79.73	85.19	82.83	82.42	83.46	82.94
		VCD	86.15	85.18	87.53	86.34	84.11	82.21	87.05	84.56
		IFCD (OURS)	87.30	89.54	84.47	86.93	85.83	93.10	77.40	84.58
GQA	POPULAR	REGULAR	79.90	80.85	78.36	79.59	76.19	72.16	85.28	78.17
		ICD	82.5	84.40	79.73	82.00	77.23	74.21	83.46	78.56
		VCD	81.85	78.60	87.53	82.82	79.80	76.00	87.05	81.15
		IFCD (OURS)	84.10	84.17	84.00	84.08	83.17	87.21	77.73	82.20
	ADVERSARIAL	REGULAR	74.04	72.08	78.49	75.15	70.71	65.91	85.83	75.56
		ICD	76.70	75.08	79.93	77.43	72.20	68.07	83.6	75.04
		VCD	74.97	70.01	87.36	77.73	74.33	69.46	86.87	77.19
		IFCD (OURS)	77.67	74.73	83.60	78.91	77.97	77.99	77.93	77.96
GQA	RANDOM	REGULAR	83.73	87.16	79.12	82.95	79.65	77.14	84.29	80.56
		ICD	86.10	90.38	80.80	85.32	82.30	81.94	82.87	82.40
		VCD	86.65	84.85	89.24	86.99	83.69	81.84	86.61	84.16
		IFCD (OURS)	87.97	90.94	84.33	87.51	84.77	92.50	75.67	83.24
	POPULAR	REGULAR	78.17	77.64	79.12	78.37	73.87	69.63	84.69	76.42
		ICD	80.00	79.53	80.80	80.16	74.70	71.23	82.87	76.61
		VCD	80.73	76.26	89.24	82.24	78.57	74.62	86.61	80.17
		IFCD (OURS)	79.76	77.61	83.67	80.52	80.13	82.90	75.93	79.26
GQA	ADVERSARIAL	REGULAR	75.08	73.19	79.16	76.06	70.56	66.12	84.33	74.12
		ICD	77.47	76.08	80.13	78.05	72.27	68.43	82.67	74.88
		VCD	76.09	70.83	88.75	78.78	75.08	70.59	85.99	77.53
		IFCD (OURS)	79.03	76.57	83.67	79.96	78.00	79.49	75.47	77.62

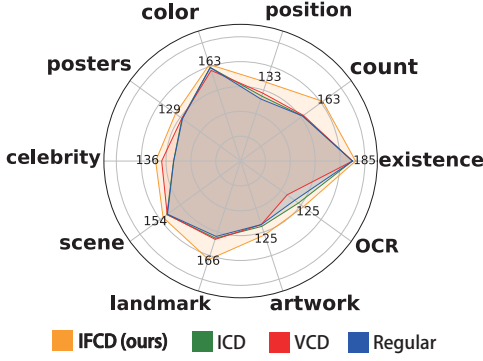


Figure 4. Perception subset of MME results on LLaVA 1.5. Regular denotes the direct sampling method, whereas ICD refers to the Instruction Contrastive Decoding, VCD refers to the Visual Contrastive Decoding baseline and IFCD is a sampling from our proposed contrastive decoding.

While direct decoding degrades by 7.8, and VCD and ICD degrade by 8.7 and 8.1, respectively, IFCD performs only a 6.8 degradation on average. The performance improvement and smaller performance degradation scale show the effectiveness and stability of IFCD.

Results on MME To evaluate LVLMs on diverse perceptual

tasks, complement POPE’s focus on object existence, and enable a broader performance assessment, we experiment on MME. As shown in Figure 4, there is a general improvement in perception-related tasks with the application of IFCD. Table 2 provides a more detailed comparison within the subset of object hallucination tasks in the MME. IFCD proves effective in attenuating the overall hallucination rate of the LVLMs, resulting in a 7.6% and 13.8% increase in the total score of InstructBLIP and LLaVA 1.5 respectively. Specifically, there is a notable increase in count and color tasks, suggesting that LVLMs are particularly susceptible to mistakes in these areas. Editing the internal representations proves to be an effective method for inducing hallucinations in these contexts. Therefore these errors can be mitigated through contrastive decoding to address object hallucination. In contrast, the position score is relatively low across four metrics, with minimal uplift from IFCD, suggesting the relatively weak ability of LVLMs in position reasoning. We demonstrate and discuss the performance of MME in more detail in Appendix C.

Results on MSCOCO We select MSCOCO for the text generation task due to its diverse, multidomain content, which better reflects LVLMs’ susceptibility to object hal-

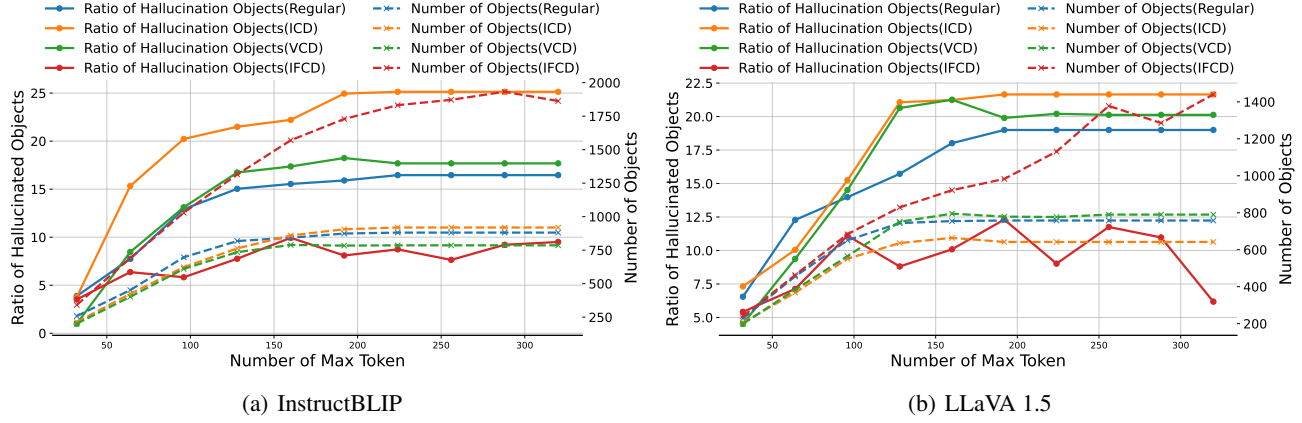


Figure 5. Comparison IFCD and regular decoding on the ratio of hallucination objects ($CHAIR_i$) with respect to the number of max tokens. IFCD maintains a low ratio of hallucination objects while increasing the number of objects.

Table 2. Results on object hallucination subset of MME on three decoding methods. The champion is marked by **bold** and **orange**, and the runner-up is marked by **cyan**.

MODEL	DECODING	OBJECT-LEVEL		ATTRIBUTE-LEVEL		TOTAL SCORES
		EXISTENCE	COUNT	POSITION	COLOR	
INSTRUCTBLIP	REGULAR	180	73.3	76.7	108.3	438.3
	ICD	180	80	80	130.3	470.3
	VCD	190	65	58.3	130	443.3
	IFCD (OURS)	185	85	63.3	138.3	471.6
LLAVA 1.5	REGULAR	180	123.3	105	158.3	566.6
	ICD	180	123.3	110	158.3	571.6
	VCD	180	125	115	153.3	573.3
	IFCD (OURS)	185	163.3	133.3	163.3	644.9

lucination. This provides a distinct evaluation from the yes/no tasks of POPE and MME. Table 3 compares IFCD with baseline methods on the image caption generation task with the prompt: “Please describe this image in detail.”. IFCD significantly reduces the proportion of hallucinated objects and sentences, with average reductions of 4.5% and 21.6% compared with direct decoding, respectively. Meanwhile, the quality of text generation in the LVLM remains at an average level, indicating that IFCD effectively balances hallucination mitigation with maintaining text generation quality.

Table 3. Results of InstructBLIP and LLaVA 1.5 on MSCOCO to demonstrate the capacity of IFCD in long-form text generation. **Bold** and **orange** indicate the best results.

MODEL	METHOD	CHAIR _s ↓	CHAIR _i ↓	BLEU↑
		REGULAR	48	13.9
INSTRUCTBLIP	ICD	58.2	18.5	8.4
	VCD	54.8	16.2	9.1
	IFCD (OURS)	39.6	11.2	8.4
	REGULAR	20	15.2	9
LLAVA 1.5	ICD	50.8	16.9	8.5
	VCD	21.8	11	10.8
	IFCD (OURS)	13.2	5.6	8

Furthermore, we also investigate the performance of IFCD under different maximum generation length settings. Figure 5 illustrates the number of objects generated (dashed line) and the ratio of hallucinated objects (solid line) for 100 ran-

domly selected images from the MSCOCO 2014 validation split. This experiment provides a comprehensive evaluation of IFCD’s robustness. Intuitively, an increase in the number of generated objects would typically correspond to a parallel increase in the hallucinatory objects. However, IFCD effectively maintains a low level of object hallucination ratios, even as the number of generated objects continues to grow. These results highlight the generalizability and effectiveness of IFCD in diverse task types, including truthfulness classification and text generation.

Case Study on LLaVA-Bench We conduct a qualitative experiment on LLaVA-Bench to demonstrate the performance of IFCD directly. The results of LLaVA-Bench are shown in Appendix D due to the space limits. In each case, we compare baseline methods and IFCD. Then the hallucination contents are marked by red. It is worth noting that IFCD provides rich information while reducing the ratio of hallucinated objects, confirming its robustness.

5. Analysis and Ablation Studies

Ablation Study The core of implementing IFCD lies in identifying the two token distributions employed for contrast, which must have a gap in the hallucination level. This enables the contrastive decoding to effectively subtract the high hallucination level portion of the distribution, thereby mitigating the object hallucinations in the final token distribution. In IFCD, we designate the distribution that undergoes anti-hallucinations as P^+ and the distribution outputted by hallucination-inducing as P^- . To validate the effectiveness and stability of IFCD, we conduct ablation experiments that comprehensively compare the results generated by various combinations of these distributions.

In Table 4, we conduct the ablation study on the combinations of distributions, showing the effectiveness and robustness of IFCD. Specifically, contrastive decoding with nega-

tive editing and original distribution is a competitive method, which could be attributed to the effect of hallucination-inducing from internal representation editing. In addition, since TruthX could be used to mitigate object hallucinations alone, IFCD overperforms it by a wide margin, manifesting the effectiveness of IFCD. Among all LVLMs, IFCD consistently demonstrates effectiveness and robustness in maintaining a low ratio of hallucination.

Table 4. Ablation of IFCD components. “EDITING”: decoding with positive editing without contrastive decoding; “w/o NEG”: contrastive decoding with positive editing and original distribution; “w/o POS”: contrastive decoding with negative editing and original distribution. The best performance is marked by **bold** and **orange**, and the second one is marked by **cyan**.

MODEL	METHOD	CHAIR _s ↓	CHAIR _i ↓
INSTRUCTBLIP	EDITING	57	15
	IFCD w/o NEG	71	19.9
	IFCD w/o POS	28	7.6
	IFCD (OURS)	39.6	11.2
LLAVA 1.5	EDITING	27	9.4
	IFCD w/o NEG	44	11.8
	IFCD w/o POS	46	14
	IFCD (OURS)	13.2	5.6

Internal Representation Editing The initial step of IFCD involves internal representation editing, making editing strength and the number of editing layers critical hyperparameters. Thus, we examine the impact of varying editing strength and the number of editing layers on IFCD performance with metrics CHAIR_s and CHAIR_i.

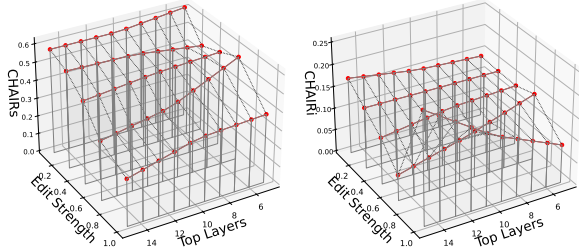


Figure 6. CHAIR scores vary with editing strength and layers.

Figure 6 presents the impact of editing strength and layers when editing the internal representation on the effectiveness of IFCD in hallucinations mitigation. For the CHAIR_s metric, the results demonstrate continuous optimization as both the editing strength and the number of editing layers increase. However, regarding the CHAIR_i metric, performance degradation occurs when the editing strength reaches 1. Furthermore, the relationship between CHAIR_i and the number of editing layers becomes inversely correlated. This observation strongly suggests that an editing strength of 1 is a critical threshold, beyond which further adjustments to

the internal representation yield diminishing performance.

Contrastive Decoding Strength After internal representation editing, contrastive decoding is employed to recalibrate distribution. During this stage, the key parameter is contrastive decoding strength α , which controls the extent of contrastive decoding. Intuitively, when the gap of distributions involved in contrast is small, larger α is needed, and vice versa.

As shown in the left part of Figure 7, the small α leads top performance, denoting the gap of distributions involved in contrastive decoding is striking, and editing internal representation is a promising way to expose LVLMs’ hallucinations preference.

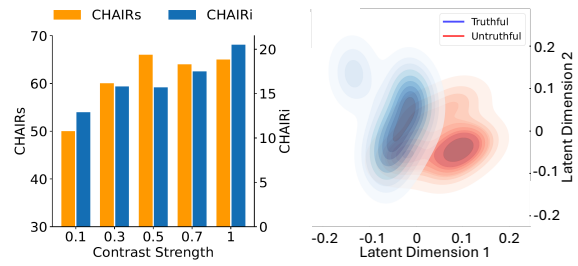


Figure 7. IFCD performance with different contrast strengths and the capacity of identifying truthfulness. The order of magnitude of the PCA figure is 10^{-7} .

The Capacity of Editing Internal Representation To investigate the effect of editing internal representations, we explore the latent space of TruthEnc(\cdot), which maps and edits the internal representation of LVLMs in latent space. We provide responses that differ in truthfulness to the LVLMs and map internal representations with different truthfulness generated during the inference process into the latent space of TruthEnc(\cdot). We then apply Principal Component Analysis (PCA) to reduce the dimensionality of the latent space to two dimensions to visualize the latent space as illustrated in the right part of Figure 7. The figure clearly illustrates a distinct separation between internal representations that differ in truthfulness, demonstrating the model’s ability to effectively identify and modify internal representations. This observation also suggests that only a minimal contrastive decoding strength is required to achieve optimal performance.

6. Conclusion

In this paper, we propose a novel method, IFCD, to mitigate object hallucination. In this method, we apply contrastive decoding based on truthfulness editing of internal representations to eliminate hallucinatory elements that are actively induced and closely aligned with statistic biases. Extensive experimentation across diverse benchmarks and LVLMs confirms the efficacy of IFCD.

References

Achiam, J., Adler, S., Agarwal, S., Ahmad, L., Akkaya, I., Aleman, F. L., Almeida, D., Altenschmidt, J., Altman, S., Anadkat, S., et al. Gpt-4 technical report. *arXiv preprint arXiv:2303.08774*, 2023.

Asai, A., Wu, Z., Wang, Y., Sil, A., and Hajishirzi, H. Self-rag: Self-reflective retrieval augmented generation. In *NeurIPS 2023 Workshop on Instruction Tuning and Instruction Following*, 2023.

Bai, J., Bai, S., Yang, S., Wang, S., Tan, S., Wang, P., Lin, J., Zhou, C., and Zhou, J. Qwen-vl: A frontier large vision-language model with versatile abilities. *arXiv preprint arXiv:2308.12966*, 2023.

Biten, A. F., Gómez, L., and Karatzas, D. Let there be a clock on the beach: Reducing object hallucination in image captioning. In *Proceedings of the IEEE/CVF Winter Conference on Applications of Computer Vision*, pp. 1381–1390, 2022.

Chen, S., Xiong, M., Liu, J., Wu, Z., Xiao, T., Gao, S., and He, J. In-context sharpness as alerts: An inner representation perspective for hallucination mitigation. In *ICLR 2024 Workshop on Reliable and Responsible Foundation Models*, 2024a.

Chen, S., Xiong, M., Liu, J., Wu, Z., Xiao, T., Gao, S., and He, J. In-context sharpness as alerts: An inner representation perspective for hallucination mitigation. In *ICLR 2024 Workshop on Reliable and Responsible Foundation Models*, 2024b. URL <https://openreview.net/forum?id=24U6vAHnYM>.

Chen, Z., Zhao, Z., Luo, H., Yao, H., Li, B., and Zhou, J. Halc: Object hallucination reduction via adaptive focal-contrast decoding. In *Forty-first International Conference on Machine Learning*, 2024c.

Chiang, W.-L., Li, Z., Lin, Z., Sheng, Y., Wu, Z., Zhang, H., Zheng, L., Zhuang, S., Zhuang, Y., Gonzalez, J. E., et al. Vicuna: An open-source chatbot impressing gpt-4 with 90%* chatgpt quality. See <https://vicuna.lmsys.org> (accessed 14 April 2023), 2(3):6, 2023.

Dhuliawala, S., Komeili, M., Xu, J., Raileanu, R., Li, X., Celikyilmaz, A., and Weston, J. Chain-of-verification reduces hallucination in large language models. In Ku, L.-W., Martins, A., and Srikumar, V. (eds.), *Findings of the Association for Computational Linguistics: ACL 2024*, pp. 3563–3578, Bangkok, Thailand, August 2024. Association for Computational Linguistics. doi: 10.18653/v1/2024.findings-acl.212. URL <https://aclanthology.org/2024.findings-acl.212/>.

Dosovitskiy, A., Beyer, L., Kolesnikov, A., Weissenborn, D., Zhai, X., Unterthiner, T., Dehghani, M., Minderer, M., Heigold, G., Gelly, S., Uszkoreit, J., and Houlsby, N. An image is worth 16x16 words: Transformers for image recognition at scale. In *International Conference on Learning Representations*, 2021. URL <https://openreview.net/forum?id=YicbFdNTTy>.

Driess, D., Xia, F., Sajjadi, M. S. M., Lynch, C., Chowdhery, A., Ichter, B., Wahid, A., Tompson, J., Vuong, Q., Yu, T., Huang, W., Chebotar, Y., Sermanet, P., Duckworth, D., Levine, S., Vanhoucke, V., Hausman, K., Toussaint, M., Greff, K., Zeng, A., Mordatch, I., and Florence, P. PaLM-e: An embodied multimodal language model. In Krause, A., Brunskill, E., Cho, K., Engelhardt, B., Sabato, S., and Scarlett, J. (eds.), *Proceedings of the 40th International Conference on Machine Learning*, volume 202 of *Proceedings of Machine Learning Research*, pp. 8469–8488. PMLR, 23–29 Jul 2023. URL <https://proceedings.mlr.press/v202/driess23a.html>.

Fu, C., Chen, P., Shen, Y., Qin, Y., Zhang, M., Lin, X., Yang, J., Zheng, X., Li, K., Sun, X., et al. Mme: A comprehensive evaluation benchmark for multimodal large language models. *arXiv preprint arXiv:2306.13394*, 2023.

Han, J., Kossen, J., Razzak, M., Schut, L., Malik, S. A., and Gal, Y. Semantic entropy probes: Robust and cheap hallucination detection in llms. In *ICML 2024 Workshop on Foundation Models in the Wild*, 2024.

Hu, X., Ru, D., Qiu, L., Guo, Q., Zhang, T., Xu, Y., Luo, Y., Liu, P., Zhang, Y., and Zhang, Z. Knowledge-centric hallucination detection. In Al-Onaizan, Y., Bansal, M., and Chen, Y.-N. (eds.), *Proceedings of the 2024 Conference on Empirical Methods in Natural Language Processing*, pp. 6953–6975, Miami, Florida, USA, November 2024. Association for Computational Linguistics. doi: 10.18653/v1/2024.emnlp-main.395. URL <https://aclanthology.org/2024.emnlp-main.395/>.

Ji, Z., Lee, N., Frieske, R., Yu, T., Su, D., Xu, Y., Ishii, E., Bang, Y. J., Madotto, A., and Fung, P. Survey of hallucination in natural language generation. *ACM Computing Surveys*, 55(12):1–38, 2023.

Leng, S., Zhang, H., Chen, G., Li, X., Lu, S., Miao, C., and Bing, L. Mitigating object hallucinations in large vision-language models through visual contrastive decoding. In *Proceedings of the IEEE/CVF Conference on Computer Vision and Pattern Recognition*, pp. 13872–13882, 2024.

Li, D., Li, J., Le, H., Wang, G., Savarese, S., and Hoi, S. C. LAVIS: A one-stop library for language-vision intelligence. In Bollegala, D., Huang, R., and Ritter,

A. (eds.), *Proceedings of the 61st Annual Meeting of the Association for Computational Linguistics (Volume 3: System Demonstrations)*, pp. 31–41, Toronto, Canada, July 2023a. Association for Computational Linguistics. doi: 10.18653/v1/2023.acl-demo.3. URL <https://aclanthology.org/2023.acl-demo.3/>.

Li, J., Li, D., Savarese, S., and Hoi, S. Blip-2: Bootstrapping language-image pre-training with frozen image encoders and large language models. In *International conference on machine learning*, pp. 19730–19742. PMLR, 2023b.

Li, X. L., Holtzman, A., Fried, D., Liang, P., Eisner, J., Hashimoto, T., Zettlemoyer, L., and Lewis, M. Contrastive decoding: Open-ended text generation as optimization. In Rogers, A., Boyd-Graber, J., and Okazaki, N. (eds.), *Proceedings of the 61st Annual Meeting of the Association for Computational Linguistics (Volume 1: Long Papers)*, pp. 12286–12312, Toronto, Canada, July 2023c. Association for Computational Linguistics. doi: 10.18653/v1/2023.acl-long.687. URL <https://aclanthology.org/2023.acl-long.687/>.

Li, Y., Du, Y., Zhou, K., Wang, J., Zhao, X., and Wen, J.-R. Evaluating object hallucination in large vision-language models. In Bouamor, H., Pino, J., and Bali, K. (eds.), *Proceedings of the 2023 Conference on Empirical Methods in Natural Language Processing*, pp. 292–305, Singapore, December 2023d. Association for Computational Linguistics. doi: 10.18653/v1/2023.emnlp-main.20. URL <https://aclanthology.org/2023.emnlp-main.20/>.

Lin, T.-Y., Maire, M., Belongie, S., Hays, J., Perona, P., Ramanan, D., Dollár, P., and Zitnick, C. L. Microsoft coco: Common objects in context. In Fleet, D., Pajdla, T., Schiele, B., and Tuytelaars, T. (eds.), *Computer Vision – ECCV 2014*, pp. 740–755, Cham, 2014. Springer International Publishing. ISBN 978-3-319-10602-1.

Liu, H., Li, C., Wu, Q., and Lee, Y. J. Visual instruction tuning. *Advances in neural information processing systems*, 36, 2024.

Mahaut, M., Aina, L., Czarnowska, P., Hardalov, M., Müller, T., and Marquez, L. Factual confidence of LLMs: on reliability and robustness of current estimators. In Ku, L.-W., Martins, A., and Srikumar, V. (eds.), *Proceedings of the 62nd Annual Meeting of the Association for Computational Linguistics (Volume 1: Long Papers)*, pp. 4554–4570, Bangkok, Thailand, August 2024. Association for Computational Linguistics. doi: 10.18653/v1/2024.acl-long.250. URL <https://aclanthology.org/2024.acl-long.250/>.

Min, K., Kim, M., Lee, K.-i., Lee, D., and Jung, K. Mitigating hallucinations in lmlms via summary-guided decoding. In *Neurips Safe Generative AI Workshop 2024*, 2024.

Pal, A., Umapathi, L. K., and Sankarasubbu, M. Med-HALT: Medical domain hallucination test for large language models. In Jiang, J., Reitter, D., and Deng, S. (eds.), *Proceedings of the 27th Conference on Computational Natural Language Learning (CoNLL)*, pp. 314–334, Singapore, December 2023. Association for Computational Linguistics. doi: 10.18653/v1/2023.conll-1.21. URL <https://aclanthology.org/2023.conll-1.21/>.

Pan, K., Fan, Z., Li, J., Yu, Q., Fei, H., Tang, S., Hong, R., Zhang, H., and Sun, Q. Towards unified multi-modal editing with enhanced knowledge collaboration. In *The Thirty-eighth Annual Conference on Neural Information Processing Systems*, 2024. URL <https://openreview.net/forum?id=kf80ZS3fVy>.

Papineni, K., Roukos, S., Ward, T., and Zhu, W.-J. Bleu: a method for automatic evaluation of machine translation. In Isabelle, P., Charniak, E., and Lin, D. (eds.), *Proceedings of the 40th Annual Meeting of the Association for Computational Linguistics*, pp. 311–318, Philadelphia, Pennsylvania, USA, July 2002. Association for Computational Linguistics. doi: 10.3115/1073083.1073135. URL <https://aclanthology.org/P02-1040/>.

Radford, A., Kim, J. W., Hallacy, C., Ramesh, A., Goh, G., Agarwal, S., Sastry, G., Askell, A., Mishkin, P., Clark, J., et al. Learning transferable visual models from natural language supervision. In *International conference on machine learning*, pp. 8748–8763. PMLR, 2021.

Rafailov, R., Sharma, A., Mitchell, E., Manning, C. D., Ermon, S., and Finn, C. Direct preference optimization: Your language model is secretly a reward model. *Advances in Neural Information Processing Systems*, 36, 2024.

Rohrbach, A., Hendricks, L. A., Burns, K., Darrell, T., and Saenko, K. Object hallucination in image captioning. In Riloff, E., Chiang, D., Hockenmaier, J., and Tsujii, J. (eds.), *Proceedings of the 2018 Conference on Empirical Methods in Natural Language Processing*, pp. 4035–4045, Brussels, Belgium, October–November 2018. Association for Computational Linguistics. doi: 10.18653/v1/D18-1437. URL <https://aclanthology.org/D18-1437/>.

Sahoo, P., Meharia, P., Ghosh, A., Saha, S., Jain, V., and Chadha, A. A comprehensive survey of hallucination in large language, image, video and audio foundation models. *Findings of the Association for Computational Linguistics: EMNLP 2024*, pp. 11709–11724, 2024.

Sanderson, K. Gpt-4 is here: what scientists think. *Nature*, 615(7954):773, 2023.

Singhal, A., Law, T., Kassner, C., Gupta, A., Duan, E., Damle, A., and Li, R. Multilingual fact-checking using llms. In *Proceedings of the Third Workshop on NLP for Positive Impact*, pp. 13–31, 2024.

Song, Z. and Huang, S. Hscl-rl: Mitigating hallucinations in multimodal large language models. In *NeurIPS 2024 Workshop on Open-World Agents*, 2024.

Stiennon, N., Ouyang, L., Wu, J., Ziegler, D., Lowe, R., Voss, C., Radford, A., Amodei, D., and Christiano, P. F. Learning to summarize with human feedback. *Advances in Neural Information Processing Systems*, 33: 3008–3021, 2020.

Wang, X., Pan, J., Ding, L., and Biemann, C. Mitigating hallucinations in large vision-language models with instruction contrastive decoding. In Ku, L.-W., Martins, A., and Srikumar, V. (eds.), *Findings of the Association for Computational Linguistics: ACL 2024*, pp. 15840–15853, Bangkok, Thailand, August 2024. Association for Computational Linguistics. doi: 10.18653/v1/2024.findings-acl.937. URL <https://aclanthology.org/2024.findings-acl.937/>.

Wei, J., Bosma, M., Zhao, V., Guu, K., Yu, A. W., Lester, B., Du, N., Dai, A. M., and Le, Q. V. Finetuned language models are zero-shot learners. In *International Conference on Learning Representations*, 2022. URL <https://openreview.net/forum?id=gEZrGCozdqR>.

Wen, L., Yang, X., Fu, D., Wang, X., Cai, P., Li, X., Tao, M., Li, Y., Linran, X., Shang, D., et al. On the road with gpt-4v (ision): Explorations of utilizing visual-language model as autonomous driving agent. In *ICLR 2024 Workshop on Large Language Model (LLM) Agents*, 2024.

Wolf, T., Debut, L., Sanh, V., Chaumond, J., Delangue, C., Moi, A., Cistac, P., Rault, T., Louf, R., Funtowicz, M., et al. Transformers: State-of-the-art natural language processing. *EMNLP 2020*, pp. 38, 2020.

Yang, Z., Li, L., Wang, J., Lin, K., Azarnasab, E., Ahmed, F., Liu, Z., Liu, C., Zeng, M., and Wang, L. Mm-react: Prompting chatgpt for multimodal reasoning and action. *arXiv preprint arXiv:2303.11381*, 2023.

Ye, Q., Xu, H., Ye, J., Yan, M., Hu, A., Liu, H., Qian, Q., Zhang, J., and Huang, F. mplug-owl2: Revolutionizing multi-modal large language model with modality collaboration. In *Proceedings of the IEEE/CVF Conference on Computer Vision and Pattern Recognition (CVPR)*, pp. 13040–13051, June 2024a.

Ye, Q., Xu, H., Ye, J., Yan, M., Hu, A., Liu, H., Qian, Q., Zhang, J., and Huang, F. mplug-owl2: Revolutionizing multi-modal large language model with modality collaboration. In *Proceedings of the IEEE/CVF Conference on Computer Vision and Pattern Recognition*, pp. 13040–13051, 2024b.

Zhang, S., Yu, T., and Feng, Y. Truthx: Alleviating hallucinations by editing large language models in truthful space. In *Proceedings of the 62th Annual Meeting of the Association for Computational Linguistics (Volume 1: Long Papers)*. Association for Computational Linguistics, 2024. URL <https://arxiv.org/abs/2402.17811>.

Zhang, Y., Li, Y., Cui, L., Cai, D., Liu, L., Fu, T., Huang, X., Zhao, E., Zhang, Y., Chen, Y., et al. Siren’s song in the ai ocean: a survey on hallucination in large language models. *arXiv preprint arXiv:2309.01219*, 2023.

Zhao, L., Deng, Y., Zhang, W., and Gu, Q. Mitigating object hallucination in large vision-language models via image-grounded guidance. In *Neurips Safe Generative AI Workshop 2024*, 2024.

Zhao, W. X., Zhou, K., Li, J., Tang, T., Wang, X., Hou, Y., Min, Y., Zhang, B., Zhang, J., Dong, Z., et al. A survey of large language models. *arXiv preprint arXiv:2303.18223*, 2023.

Zhou, Y., Cui, C., Yoon, J., Zhang, L., Deng, Z., Finn, C., Bansal, M., and Yao, H. Analyzing and mitigating object hallucination in large vision-language models. In *NeurIPS 2023 Workshop on Instruction Tuning and Instruction Following*, 2023.

Zhu, D., Chen, J., Shen, X., Li, X., and Elhoseiny, M. MiniGPT-4: Enhancing vision-language understanding with advanced large language models. In *The Twelfth International Conference on Learning Representations*, 2024. URL <https://openreview.net/forum?id=1tZbq88f27>.

A. Training Effect of Internal Representation Editing Model

Training the TruthX, which assesses the truthfulness alignment of internal representations in LVLMs, is a prerequisite for the IFCD method. We train the TruthX using a uniformly sampled set of image-text pairs from the MSCOCO dataset. The specific configuration contains an image as visual information input and two counterfactual responses. For training for $\text{SemEnc}(\cdot)$ to maintain semantic consistency during internal representation editing, truthful and untruthful responses are composed of as many similar tokens as possible (Zhang et al., 2024).

Table 5. IFCD performance with different training sizes of internal representation editing model.

TRAINING SIZE	ADVERSARIAL ACC	POPULAR ACC	RANDOM ACC
100	82.1	84.7	87.4
200	76	77.3	77.6
300	83.5	86	86.4
400	82.1	83.6	85.3
500	82.3	84.2	85.5
600	80.4	81.8	82
700	75.8	77.6	79.2

The performance of TruthX in assessing the truthfulness alignment of internal representations is anticipated to improve with an increase in the size of the training dataset, thereby enhancing the efficacy of the IFCD method. However, validation results indicate that the performance of IFCD reaches its peak accuracy when the training dataset contains 300 samples. Interestingly, further increases in the training data size beyond this threshold result in a decline in IFCD’s performance. This decline may be attributed to potential overfitting or the introduction of noise within the additional data.

We compare the performance of IFCD with varying training sizes on the MSCOCO subset of POPE, utilizing three different POPE sampling strategies. The results remain consistent across all strategies. As shown in the left part of Figure 5, when conducting IFCD on LLaVA 1.5 using TruthX models trained with different amounts of training data, it is visually evident that the overall best performance is achieved when the training data size reaches 300 in POPE. Further increasing the training data, however, leads to a significant decline in performance.

B. Experiments Details

The overall experiment settings are reported in Table 6. While regular direct decoding follows this setting in each experiment, baseline method VCD and our proposed IFCD follow specific settings. We use the default code for the implementation of two backbone LVLMs, InstructBLIP and LLaVA 1.5 in HuggingFace Transformers Repository (Wolf et al., 2020).

The hyper-parameters settings for IFCD in our experiments in Section 4 is reported in Table 7. Specifically, as we discussed in Section 5, there are three major hyper-parameters that actively adjust the effectiveness of IFCD: *Editing Strength*, *Editing Layers*, and *Contrastive Decoding Strength*.

Regarding the comparison of baseline decoding methods VCD and ICD, we adopt the code, and hyper-parameters in the public repositories and papers. We strictly follow the implementation as reported in the paper to reproduce results as Table 8 (VCD) and Table 9 (ICD).

Table 6. Overall Experiment Settings.

PARAMETERS	VALUE
MAXIMUM NEW TOKEN (POPE)	32
MAXIMUM NEW TOKEN (MME)	32
MAXIMUM NEW TOKEN (MSCOCO)	128
MAXIMUM NEW TOKEN (LLAVA-BENCH)	512
TEMPERATURE	1
TOP-K	FALSE
TOP-P	1

Table 7. IFCD Hyperparameter Settings.

PARAMETERS	VALUE
EDITING STRENGTH	0.5
EDITING LAYERS	15
CONTRASTIVE DECONDING STRENGTH	0.1
ADAPTIVE PLAUSIBLE THRESHOLD	0.1

Table 8. VCD Hyperparameter Settings.

PARAMETERS	VALUE
NOISE STEP (POPE)	999
NOISE STEP (EXCEPT POPE)	500
CONTRASTIVE DECONDING STRENGTH	1
ADAPTIVE PLAUSIBLE THRESHOLD	0.1

Table 9. ICD Hyperparameter Settings.

PARAMETERS	VALUE
INSTRUCTION DIRTURBANCE PROMPT	“YOU ARE A CONFUSED OBJECT DETECTOR.”
CONTRASTIVE DECODING STRENGTH	1
ADAPTIVE PLAUSIBLE THRESHOLD	0.1

C. MME Experiment detailed Results

In Table 10, we comprehensively present the performance of two LVLM benchmarks on perception-related tasks within the MME benchmark. The results demonstrate that the baseline models exhibit consistent performance patterns, while the employment of IFCD significantly enhances their overall perception capabilities. This improvement is likely attributed to IFCD’s ability to effectively mitigate logits that expose object hallucination, thereby recalibrating the LVLM to prioritize visual information rather than relying on pre-existing biases and priors. In contrast, the position, celebrity, and OCR score of IFCD is at a relatively low level on InstructBLIP, while LLaVA 1.5 with IFCD achieves the highest scores on each task among the three decoding methods, suggesting the comparatively weak ability of specific LVLM in these reasoning tasks.

Table 10. Results on all MME perception-related tasks. The best performance of each setting is marked by **bold** and **orange**. The second is marked by **cyan**.

MODEL	DECODING	EXISTENCE	COUNT	POSITION	COLOR	POSTERS	CELEBRITY	SCENE	LANDMARK	ARTWORK	OCR	TOTAL SCORE
INSTRUCTBLIP	REGULAR	180	73.3	76.6	108.3	123.4	105.5	144.75	126.25	99.25	95	1037.35
	ICD	180	80	80	130.3	116.6	97.3	151	133	101	70	1072.2
	VCD	190	65	58.3	130	135	102.9	152.25	143.75	87	65	1064.2
	IFCD	185	85	63.3	138.3	144.5	103.5	163.5	160.75	101	80	1144.85
LLAVA 1.5	REGULAR	180	123.3	105	158.3	115.6	107.6	145.5	127.5	107.5	107.5	1170.3
	ICD	180	123.3	110	158.3	116.6	107.9	146.75	130.5	110.5	115	1183.85
	VCD	180	125	115	153.3	117	127	146	132.5	107.5	92.5	1203.3
	IFCD	185	163.3	133.3	163.3	129.6	136.7	154.25	166.75	125	125	1357.2

D. Experiment Results on LLaVA-Bench

As discussed in Section 4.2, we leverage LLaVA-Bench as a case study to compare the outputs of IFCD with other methods qualitatively. All methods use the settings as Section 4.1. In all cases, red fonts indicate object hallucination, including object existence, attribute, or relationship hallucination.



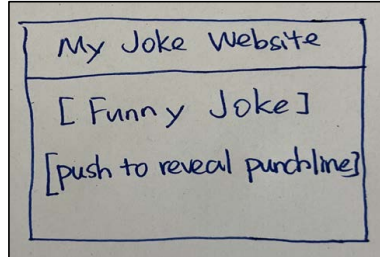
Prompt: Describe this photo in detail.

Regular Decoding: The image features a delicious-looking sandwich on display, with two halves of a sub sandwich cut in half. The sandwich is filled with various meats, including ham and bacon, as well as vegetables such as lettuce and tomatoes. The sandwich is presented on a black background, showcasing its fresh and appetizing appearance. **The sandwich is placed on a table, with a cutting board nearby, which suggests that it is ready to be consumed. The sandwich is also accompanied by a bottle of water, which adds to the overall presentation.**

Instruction Contrastive Decoding: In the image, there is a sandwich cut in half, showcasing its contents, placed on a black surface. The sandwich has a visible lettuce topping and meat inside, which is visible from different parts of the image. **There are multiple sandwich halves, some positioned closer to the top left corner and others scattered throughout the picture, with some closer to the center. The sandwiches appear to have a strong presence in the photo, capturing the attention of viewers.**

Visual Contrastive Decoding: The image features a delicious sandwich cut into two pieces, placed on a black background. The sandwich is composed of a sub-like bread filled with various ingredients, such as lettuce, tomato, and meat. The sandwich is cut in half and appears to be a fresh, homemade meal. There are multiple sandwich slices on the table, each one showcasing the mouthwatering ingredients. **The sandwich is accompanied by a large bowl on the right side of the image. The bowl is filled with what appears to be a green salad, perhaps a perfect complement to the sandwich.**

Internal Fact-based Contrastive Decoding: The image features a display of a sub sandwich with two halves, each containing a variety of meats and vegetables. The display showcases a sub sandwich with a cut in the middle, revealing a delicious-looking filling of meats and vegetables. The meats used in the display include ham, bacon, and a roast beef, which are all prominently displayed. Various vegetables can be seen as well, including lettuce, tomatoes, and onions. The overall presentation of the sub sandwich is visually appealing and inviting, showcasing the quality and variety of ingredients used in the sandwich.



Prompt: Describe this photo in detail.

Regular Decoding: The image features a handwritten note on a piece of paper, which reads "My joke website: I funny joke. I funny joke. I funny joke." The note is accompanied by a drawing of **a hand, which is holding a pen and writing the text. The hand is positioned on the left side of the paper**, and the text is written in a neat and organized manner. The handwriting is clear and easy to read.

Instruction Contrastive Decoding: In the image, there is a white piece of paper with a blue ink handwriting that reads "My joke website. i funny joke i funny pun i push to reveal punchline". The writing is spread out across the paper, with the first three words appearing on the top, followed by the rest of the text below. There are **multiple instances of the word "i" scattered throughout the text, possibly emphasizing the word in the joke. Additionally, there are several smaller handwritten notes appearing on the page, such as two near the top left and one near the top right.**

Visual Contrastive Decoding: The image features **a drawing of a web page**, with the title "My Joke Website". The drawing consists of a single line with two words, "funny joke" written in the top part, **followed by "funny jokes" in the bottom part**. The drawing is accompanied by a caption, which reads "PUSH TO REVEAL PUNCHING". **The text appears on a separate layer above the joke. Additionally, there are two smaller captions placed at the bottom of the drawing, with one located close to the left edge and the other near the right edge.** These captions provide additional context and information about the drawing.

Internal Fact-based Contrastive Decoding: The photo features a handwritten note that reads "my joke website pushing to reveal punching" on a piece of paper. The note mentions a joke website, which suggests that there is a sense of humor involved in the process. The handwriting and the words "pushing" and "reveal" suggest that there is a sense of urgency and a desire to reveal something. The handwriting also includes various words and phrases, such as "pushing" and "reveal," which suggests a sense of urgency and a desire to reveal something.

Figure 8. LLaVA-Bench results comparing direct decoding, ICD, VCD, and IFCD with InstructBLIP backbone.



Prompt: Describe this photo in detail.

Regular Decoding: The image depicts a colorful scene featuring a dining table filled with various pastries and plates of food. Surrounding the table are three different animals: **two bears** and a hare. Separated into distinct groups, one bear is positioned on the left side toward the center of the table, **while the other bear is situated on the right side**, near the edge of the table. The hare is present in the foreground, sitting opposite the bears. In this charming setting, each animal appears to be enjoying a snack or a treat as they eat the delicious food. **A "cake" can be seen on the plate in front of the bears**, while there are also **two bowls and two spoons on the table**, indicating that the animals are being attended to.

Visual Contrastive Decoding: The image features three animals sitting around a dining table, enjoying a meal together. One of the animals is a bear, another a rabbit, and the third is a cat. The table is filled with a variety of food items, including cakes, donuts, and cups, as well as spoons for utensils. There are **five cakes** scattered across the table, with some located near the center and **others positioned towards the edge of the table**. A couple of **donuts** can be seen on the table as well. **The rabbit is on the left side**, while **the bear is situated in the middle**, and **the cat is on the right side of the table**. All the animals appear to be sharing the meal and enjoying the company of one another.

Visual Contrastive Decoding: The image features three animals sitting around a small wooden table, enjoying a meal together. One animal appears to be a rabbit, while another is a cat, and the third is a bear. Each animal has its own plate of food, consisting of cookies and donuts. There are also spoons placed on the table for serving the desserts. In addition to the main trio, there are **two other smaller figures present in the scene**, possibly indicating more guests or additional food items. The overall atmosphere suggests a cozy gathering among friends or family members.

Internal Fact-based Contrastive Decoding: The image features a group of three animals sitting around a dining table, enjoying a meal together. The animals include a rabbit, a cat, and a bear. They are all seated on the grass, with the rabbit on the left side, the cat in the middle, and the bear on the right side of the table. The table is set with various food items, including a cake, a bowl, and a cup. The cake is placed in the center of the table, while the bowl and cup are positioned closer to the right side. The scene appears to be a whimsical and friendly gathering of these different animals sharing a meal.



Prompt: Describe this photo in detail.

Regular Decoding: The image portrays a man wearing an animal costume with a **Pixar dog's mask on his head**. He is holding a small, cute **teddy bear** over his **right shoulder**, playing a humorous scene. The **teddy bear**'s head is in a circle outline design on it, possibly **indicating an official or even illegal party situation is taking place**. The man is cheerfully posing with the teddy bear, creating a lively and fun atmosphere in the scene.

Instruction Contrastive Decoding: The image features a man dressed as a **cat character**, possibly resembling a crossbreed between a dog and a cat or a hyena, holding a small dog or puppy in its arms. The **cat character** seems to be happy and proudly showing off the small dog or puppy to others. They are both situated on top of a hill or cliff, creating an interesting contrast between the human character and the natural environment.

Visual Contrastive Decoding: The image features a man in a cartoon lion costume **holding** a baby Shiba Inu dog **in his arms**. The lion character is wearing a **necklace** and appears to be happy, as he is smiling. The man holding the dog seems to be enjoying the scene, creating a whimsical and heartwarming moment.

Internal Fact-based Contrastive Decoding: The image features a man, possibly Elon Musk, dressed in a monkey costume and holding a small dog in his arms. The man is smiling, and the dog appears to be enjoying the moment as well. The scene is set against a backdrop of a cloudy sky, adding to the overall atmosphere of the image.

Figure 9. LLaVA-Bench results comparing direct decoding, ICD, VCD, and IFCD with LLaVA 1.5 backbone.